

Arsenic Induced Mitochondrial DNA Damage and Altered Mitochondrial Oxidative Function: Implications for Genotoxic Mechanisms in Mammalian Cells

Michael A. Partridge,¹ Sarah X.L. Huang,^{1,3} Evelyn Hernandez-Rosa,² Mercy M. Davidson,² and Tom K. Hei^{1,3}

¹Center for Radiological Research and ²Department of Neurology, College of Physicians and Surgeons and ³Department of Environmental Health Sciences, Mailman School of Public Health, Columbia University, New York, New York

Abstract

Arsenic is a well-established human carcinogen that is chronically consumed in drinking water by millions of people worldwide. Recent evidence has suggested that arsenic is a genotoxic carcinogen. Furthermore, we have shown that mitochondria mediate the mutagenic effects of arsenic in mammalian cells, as arsenic did not induce nuclear mutations in mitochondrial DNA (mtDNA)-depleted cells. Using the human-hamster hybrid A₁ cells, we show here that arsenic alters mitochondrial function by decreasing cytochrome *c* oxidase function and oxygen consumption but increasing citrate synthase function. These alterations correlated with depletion in mtDNA copy number and increase in large heteroplasmic mtDNA deletions. In addition, mtDNA isolated periodically from cultures treated continuously with arsenic did not consistently display the same deletion pattern, indicating that the mitochondrial genome was subjected to repeated and continuous damage. These data support the theory that the mitochondria, and particularly mtDNA, are important targets of the mutagenic effects of arsenic in mammalian cells. [Cancer Res 2007;67(11):5239–47]

Introduction

Arsenic is an important environmental carcinogen that affects millions of people worldwide. In West Bengal, India, and Bangladesh alone, more than 35 million people are believed to be exposed to an arsenic concentration in drinking water exceeding 50 µg/L, the maximum allowable limit in Bangladesh (1). In contrast, the current limit in the United States and member countries of the European Union is 10 µg/L. Individuals chronically exposed to arsenic develop a range of diseases: initially keratosis of the skin and subsequently other deleterious neurologic and cardiovascular effects (2). Importantly, arsenic is also a known human carcinogen, and exposed individuals have a higher risk of developing skin, lung, liver, kidney, and bladder cancers (2). Although epidemiologic studies have clearly identified arsenic as a human carcinogen, the mechanism by which arsenic causes cancer is still poorly understood (3). Given the large number of contaminated sites that have been identified worldwide and the

scores of millions of people at risk, there is an urgent need to understand how arsenic mediates tumorigenesis.

Previous work from our laboratory has clearly established that arsenic is a chromosomal mutagen, even after short (1–5 days) treatment times (4), and that normal mitochondrial function is required for the genotoxic response to arsenic (5). Mitochondria are the energy-generating organelles of the cell, and structural and function abnormalities in mitochondria have been shown in cancer cells (6). Furthermore, mitochondria are a rich source of reactive oxygen species (ROS), and arsenic-induced genotoxic effects are also dependent on ROS (4, 7, 8). Taken together, this suggests a potential mechanism for arsenic-induced genotoxicity whereby arsenic disrupts mitochondrial function that leads to an increase in intracellular ROS, a subsequent downstream induction of reactive nitrogen species, and an increased mutagenic potential, either directly or via a decreased DNA repair capacity.

Mitochondria contain their own extra-nuclear DNA (mtDNA), which is a potentially susceptible target of various environmental mutagens/carcinogens, including the free radicals induced by the exposure of cells to ionizing radiation, asbestos fibers, and arsenic. This circular genome lacks protective histones, has only a subset of the DNA repair systems available to nuclear DNA (nDNA), and exists inside the organelle in an environment of high oxidative stress (9). Consequently, the mutation rate of mtDNA is greatly increased compared with nDNA (8), and an increase in the ROS burden induced by arsenic exposure could further increase the rate of mutation.

In humans, the incidence of a 4,977-bp deletion in mtDNA known as the “common deletion” increases with age (10, 11). Additionally, the occurrence of this deletion was four times greater in oral tissues of individuals who chewed areca nut, a major risk factor for oral and esophageal cancer, and the deletion was also induced in neuronal cells exposed to the mutagen ethidium bromide (12, 13). Furthermore, major mtDNA deletions have been identified in human prostate and breast cancers as well as numerous smaller deletions in a variety of other tumors (14–16).

An individual cell contains hundreds of mitochondria, each containing multiple copies of the mitochondrial genome (8). In addition to deletions, it is possible that a reduction in the copy number of mtDNA could alter mitochondrial function, which may also lead to increased cellular ROS. Interestingly, impairment of DNA repair and increased oxidative damage to the nuclear genome have been reported in cells depleted of mtDNA (17, 18). Furthermore, we have previously shown an increase in background nuclear mutations in mtDNA-depleted (ρ0) cells (5). Finally, all these mtDNA alterations may result in changes in mitochondrial oxidative phosphorylation (OXPHOS), and the emergence of the glycolytic phenotype over OXPHOS, a hallmark of cancer cells, may

Note: Supplementary data for this article are available at Cancer Research Online (<http://cancerres.aacrjournals.org/>).

Requests for reprints: Tom K. Hei, Center for Radiological Research, Columbia University, College of Physicians and Surgeons, 630 West 168th Street, New York, NY 10032. Phone: 212-305-8462; Fax: 212-305-3229; E-mail: tkh1@columbia.edu.

©2007 American Association for Cancer Research.
doi:10.1158/0008-5472.CAN-07-0074

be promoted by mitochondrial dysfunction (19). Therefore, we investigated the consequences of arsenic treatment on mitochondrial function and the role of mtDNA changes in mediating these effects.

Materials and Methods

Cell culture. The A_L human-hamster hybrid cells, CHOK1 cells stably expressing a single copy of human chromosome 11, were used in these studies. Chromosome 11 encodes the CD59 cell surface antigen that renders A_L cells sensitive to killing by specific monoclonal antibodies in the presence of rabbit serum complement as described previously (4, 5). Cells were maintained in Ham's F-12 medium, supplemented with 8% heat-inactivated fetal bovine serum, 25 $\mu\text{g}/\text{mL}$ gentamicin, and $2\times$ normal glycine (2×10^{-4} mol/L), at 37°C in a humidified 5% CO_2 incubator and passaged as described (4, 5).

Histochemistry. Histochemical staining for cytochrome *c* oxidase (COX) activity was done as described (20). Briefly, cells grown on glass coverslips were air-dried for 1 h at room temperature and preincubated with 1 mmol/L CoCl_2 and 50 μL of DMSO in 50 mmol/L Tris-HCl (pH 7.6), containing 10% sucrose, for 15 min at room temperature. Cells were rinsed with PBS and incubated for 6 h at 37°C with 10 mL of substrate solution

[10 mg cytochrome *c*, 10 mg diaminobenzidine, 2 mg catalase, and 25 μL DMSO in 10 mL of 0.1 mol/L phosphate buffer (pH 7.6)]. The coverslips were rinsed, mounted in glycerin-gelatin, and examined with a Zeiss microscope with bright-field optics.

Histochemistry staining was quantified by using Image J (NIH) software. Light and camera settings were standardized to get the absorbance boundary of 0 to 249 (from dark to white). Twenty-four bit color images were captured with $\times 40$ objective. Background subtraction was done on each image based on an empty field adjacent to the cell. All the samples were evaluated using the same threshold settings. The absorbance was acquired by averaging the quantitative computerized image analysis data obtained from at least 23 randomly selected cells from each sample. Statistical analysis was done with the Student's *t* test. $P < 0.05$ was considered statistically significant.

Immunofluorescence. Cells were grown on glass coverslips in growth medium until confluent and fixed (PBS, 4% paraformaldehyde for 10 min) and permeabilized (PBS, 0.5% Triton X-100 for 5 min). Cells were incubated with antibodies to pyruvate dehydrogenase (Binding Site, United Kingdom). Mitochondria were visualized with secondary antibodies from Amersham. Nuclear staining was done with propidium iodide (PharMingen). Images were captured using a laser confocal microscope (Nikon). Analysis of tubulin in cells was done as described previously (21). Briefly, cells were fixed (-20°C methanol, 10 min) and rehydrated in PBS for 5 min and stained with and

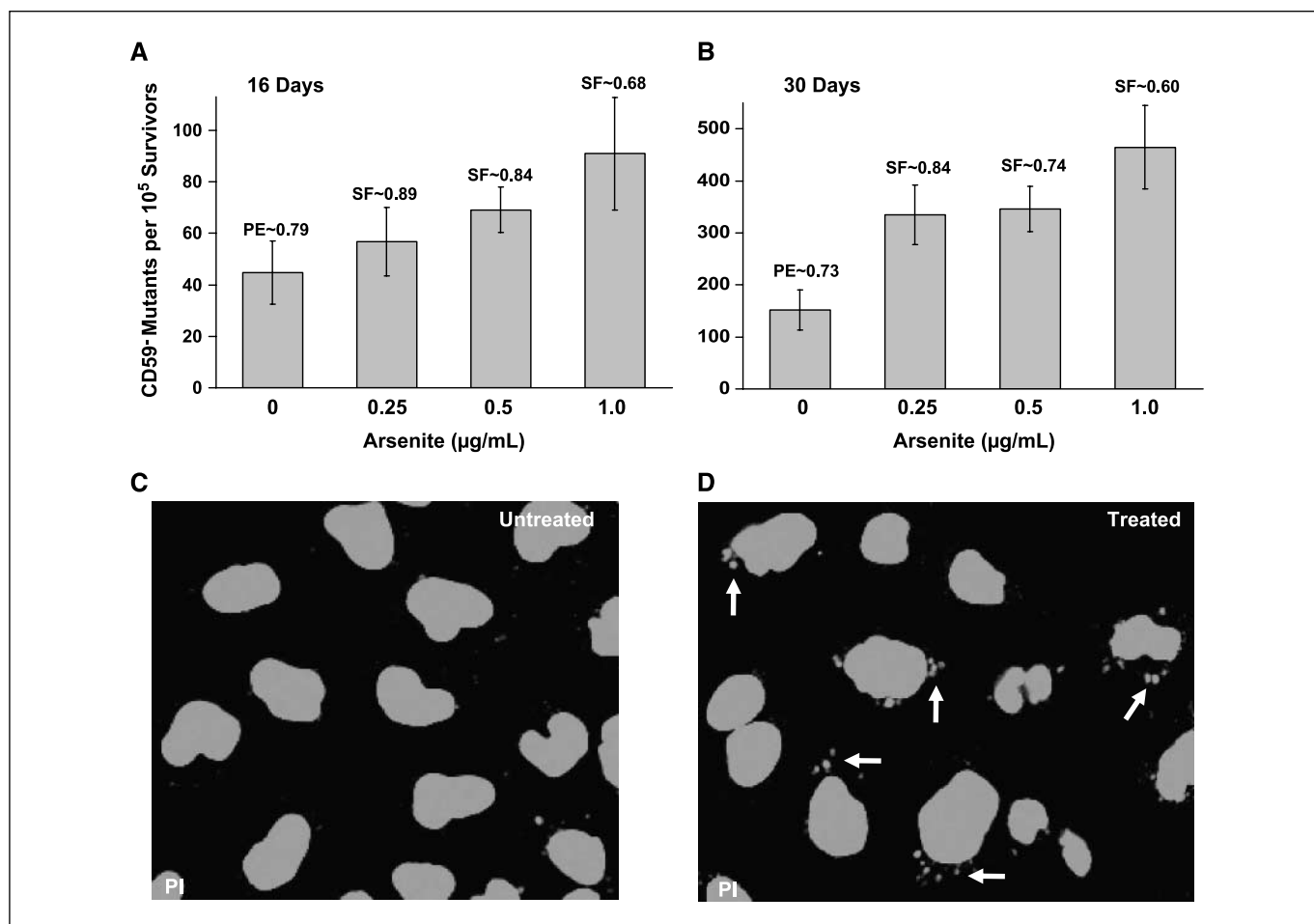


Figure 1. Cells exposed to arsenic have an increase in both CD59⁻ mutations and the incidence of micronuclei. A_L cells exposed to graded doses of sodium arsenite for the indicated times were assessed for mutations at the CD59⁻ locus (A and B). Pooled data from three experiments. PE, plating efficiency; SF, surviving fraction when compared with untreated A_L cells. Columns, CD59⁻ mutants per survivors; bars, SD. Untreated (C) and arsenic-treated (D) A_L cells were allowed to grow on coverslips for up to 2 d, fixed with 4% paraformaldehyde, and stained with propidium iodide to visualize the nucleus. Arrows in (D) indicate micronuclei formation in arsenic-treated cells. Images of five random fields were captured at low power ($\times 20$ objective). Total number of nuclei was determined using Image J (NIH) software, and those with micronuclei were scored manually.

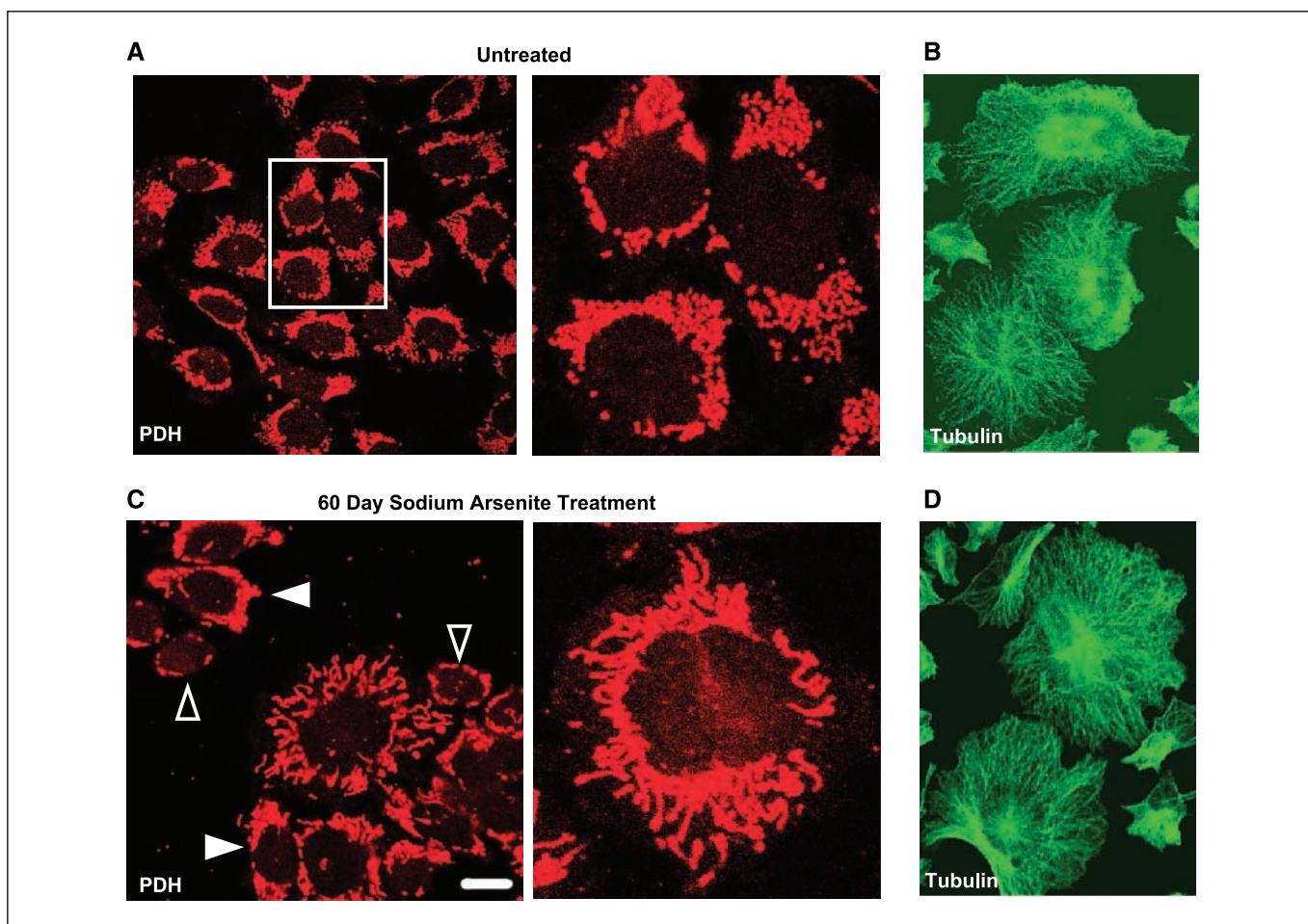


Figure 2. Sodium arsenite treatment alters the morphology of mitochondria in A_L cells. Pyruvate dehydrogenase (PDH) staining of untreated cells (A) as well as cells treated with sodium arsenite ($1 \mu\text{g}/\text{mL}$) for 60 d (C). Bar, $10 \mu\text{m}$. A, right, an enlarged image of the boxed area (left). C, closed arrowheads, cells with strong pyruvate dehydrogenase staining; open arrowheads, cells with poor staining. Right, picture of a whole cell with elongated mitochondria. B and D, tubulin staining of control cells (B) or cells exposed to arsenic ($1 \mu\text{g}/\text{mL}$) for 60 d (D).

antibody to tyrosinated tubulin (a gift from G. Gundersen, Columbia University). Secondary antibodies were from Jackson ImmunoResearch.

Determination of COX and citrate synthase activity. Biochemical assays for COX and citrate synthase activity were done as described (20). Briefly, cells in log phase of growth were trypsinized and washed with PBS, and the pellets were resuspended in reaction buffer [50 mmol/L potassium phosphate (pH 7.0)]. Cells were lysed with two cycles of freezing and thawing. Cell lysates were treated with 1.3 mmol/L lauryl maltoside before COX measurements. COX activity was assessed by measuring the oxidation of reduced cytochrome *c* at 550 nm (nmol oxidized cytochrome *c* per min per mg protein). Citrate synthase activity was assessed by measuring the reduction of 5,5'-dithiobis(2-nitrobenzoic acid) at 412 nm, coupled to the reduction of CoA by the citrate synthase reaction in the presence of oxaloacetate. The reaction was initiated by the addition of 0.5 mmol/L oxaloacetate, and the absorbance change is monitored for 2 min at 30°C . The enzyme activities were normalized to mg of protein in the cell lysate.

Oxygen consumption. Oxygen consumption in intact cells was assayed as described previously (22). Briefly, 1×10^7 cells were suspended in 1.5 mL of DMEM lacking glucose, and oxygen concentration was assayed over 3 min at 37°C in a Hansatech (MA) Clark's oxygen electrode unit.

Long-extension PCR. Total genomic DNA was extracted from exponentially growing cells according to standard techniques. Long-extension PCR was done with 50 ng of template, using LA-Taq (Takara) in a total volume of 50 μL . Samples were denatured for 5 min at 95°C followed by 30 cycles of 10 s at 98°C , 16 min at 68°C , and a final elongation for

10 min at 72°C . Forward primer, CGTAGAGTATGCTGCAGGCCCATTCG-CAC (bp 3368–3396); reverse primer, GTCTTACGCAATTTCCGGGCTCTGC-CACC (bp 2692–2663). These PCR primers were designed specifically to amplify 15,608 bp of the mtDNA, skipping only 676 bp of the *NADH1* gene. To exclude the possibility of amplifying nuclear mtDNA pseudogenes, we did the reaction on DNA from cells lacking mtDNA ($\rho 0$ cells) to ensure that no mtDNA-like sequences were amplified. Long-extension PCR products were separated by electrophoresis on a 0.8% agarose gel stained with ethidium bromide.

Real-time PCR. mtDNA copy number was determined by real-time PCR using SYBR Green detection on an Applied Biosystems 7300 Real-time PCR System (Applied Biosystems). Products amplified were a 207-bp fragment of the nuclear encoded *18S* rRNA gene (23) and a 199-bp fragment of the mtDNA encoded *12S* rRNA gene (24). The primers were as follows: 18S sense, AAGCTTGGCGTTGATTAAGTCC; 18S antisense, TAATGATCCTCCG-CAGGTTTC; 12S sense, GGGTTGGTAAATTCGTGCCAGC; and 12S antisense, CCCAGTTTGGATCTTAGCTATC. All reactions were done in triplicate. PCR conditions were as follows: 95°C for 15 min followed by 40 cycles at 95°C for 30 s, 55°C for 30 s, and 72°C for 30 s. Relative quantification of mtDNA/nDNA ratio was determined by comparative threshold cycle (C_T) method as described previously (25).

Detection of rare heteroplasmic deletions using nested PCR. A nested PCR protocol for detecting rare heteroplasmic deletions was adapted from the methods developed for detecting the common deletion in human mtDNA (26). The polymer used was Ex-Taq (Takara). PCR conditions were

as follows: denaturation for 5 min at 95°C followed by 35 cycles of 30 s at 95°C, 30 s at 55°C, and 30 s at 68°C, and a final elongation for 10 min at 72°C. Primer sets: (a) first round (5070S, CATCTAATGAGTGCAAATCAAT-TAC + 11775AS, CAGGTAAGGTCAATAGAATAAAAATAAGG); second round (5700S, GCATTCCCACGTATAAACAACATAAGC + 11387AS, GTGG-TGTTAACGTACCTCGTTGAG); (b) first round (6123S, GGTATAGTGTGAG-CAATAATGTCAATCGG + 14617AS, GTCTACAGAGAATCCCCCTCAG); second round (6716S, CTTTATAATCTGAGAAGCTTTCGC + 14154AS, GCGGGTGTTTTTTCGTATGATTGTC). Template concentrations were accurately determined using both spectrophotometric measurements and by normalizing, with serial dilutions, the intensity of ethidium bromide staining of genomic DNA in agarose gels. All deletions amplified were sequenced to determine the break points.

Results

Arsenic induced nDNA mutagenesis. To more accurately replicate normal environmental exposure conditions, we subjected cells to relatively long periods of arsenic exposure while using lower arsenic treatment levels than we had used in previous studies. Consequently, we treated cells with arsenic doses of 1, 0.5, and 0.25 $\mu\text{g}/\text{mL}$ for up to 60 days and monitored genotoxicity (CD59⁻ mutations) in the human-hamster A_L cells (CHO cells stably expressing human chromosome 11). Consistent with

previously observed mutation data, treatment of cells for 16 or 30 days resulted in a dose-dependent increase in mutation frequency (Fig. 1A and B), measured by the loss of the CD59 cell surface antigen, which is encoded by human chromosome 11 (4). This increase was also time dependent, as there was an increase in total mutations in response to increasing treatment time. Concurrently, there was a substantial increase in the background mutation rate, particularly after 60 days, which prevented precise quantification of the effect of long treatment time on CD59 mutations. Arsenic treatment also caused an almost 3-fold increase in the number of micronuclei observed in A_L cells (untreated, $11.6 \pm 2.2\%$; treated, $32.6 \pm 1.9\%$) treated for 60 days (Fig. 1C and D). Thus, arsenic exposure also resulted in genomic instability, providing further evidence that arsenic is a chromosomal mutagen.

Mitochondrial oxidative function. Given our previous findings that normal mitochondrial function was required to mediate the genotoxicity of arsenic (5), we initially analyzed changes in the morphology of the mitochondria in A_L cells after arsenic treatment by staining cells with an antibody against the mitochondrial enzyme pyruvate dehydrogenase. When examined by fluorescence microscopy, the mitochondria of untreated cells maintained a compact, punctate structure in the perinuclear region with an approximately uniform number of mitochondria from cell to cell

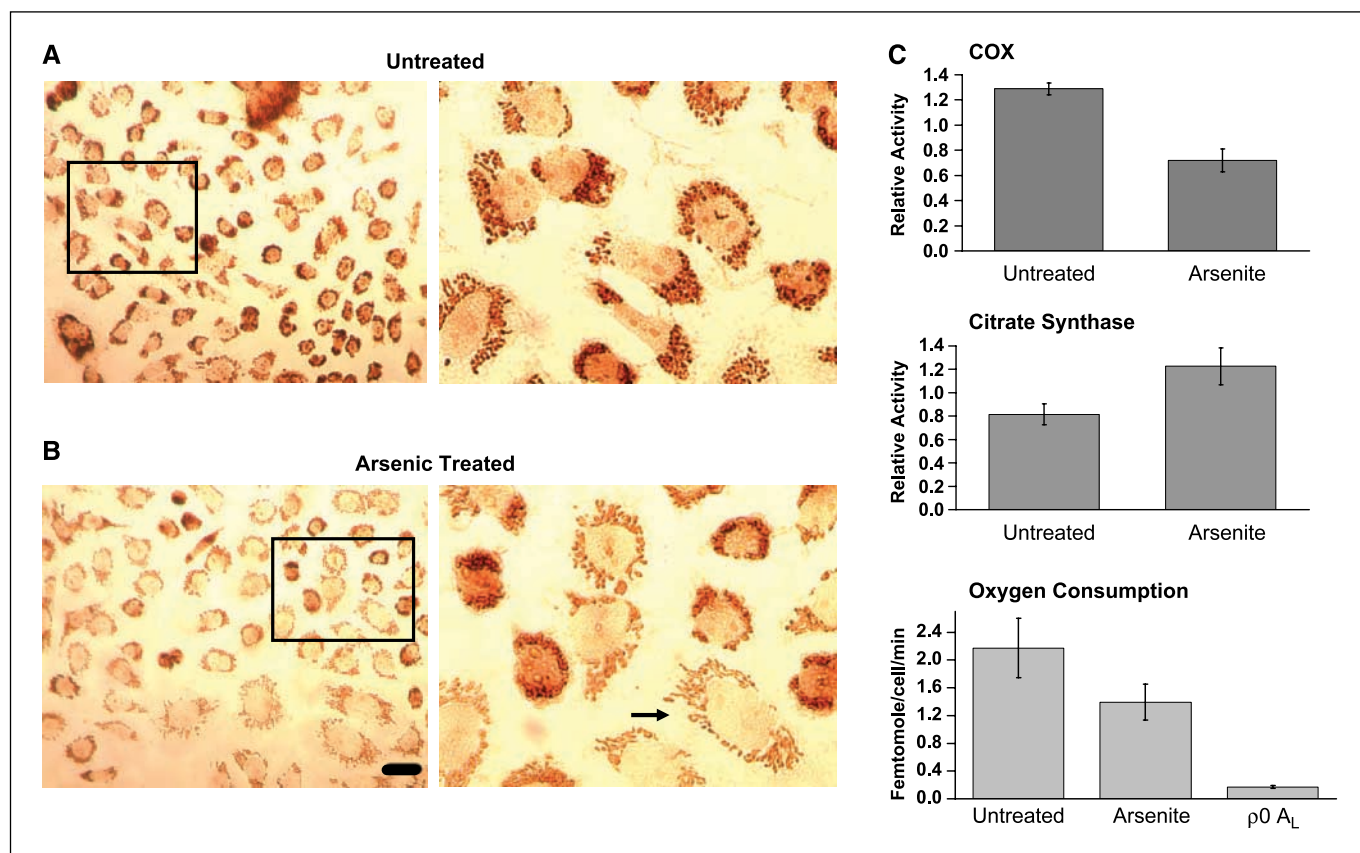
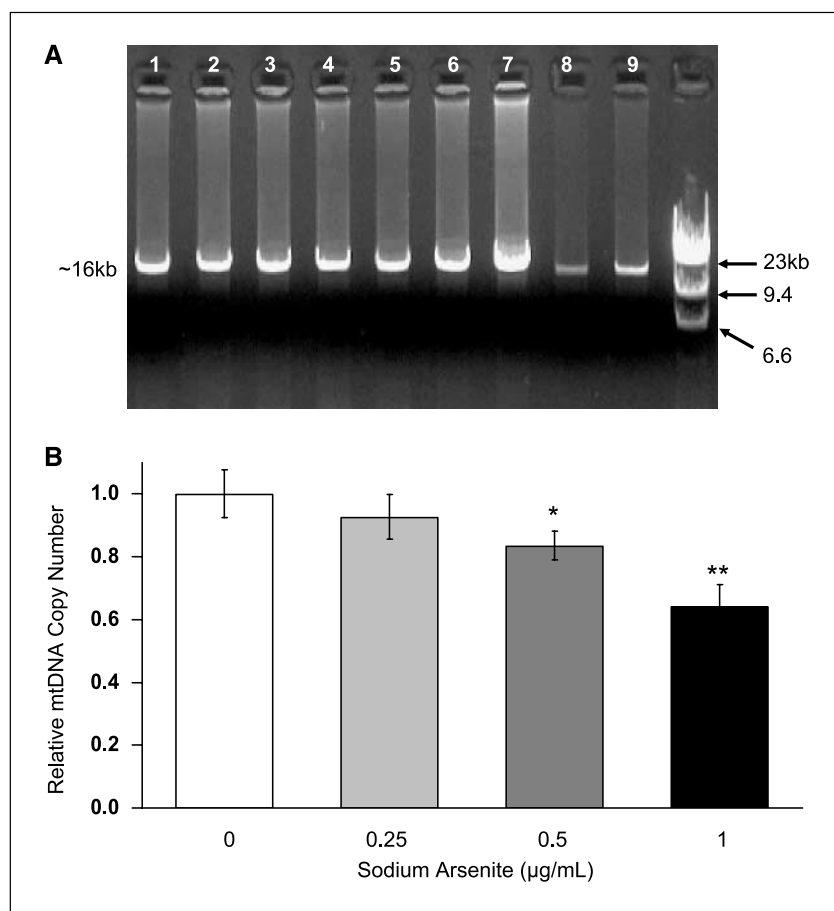


Figure 3. Analysis of COX function and oxygen consumption in control cells and those exposed to arsenic. *A*, untreated cells were grown on coverslips until confluent, air-dried, and stained for COX. *Right*, enlarged image of boxed area (*left*). *B*, cells exposed to 1 $\mu\text{g}/\text{mL}$ arsenic for 15 d were stained identically to control cells. *Bar*, 20 μm . *Right*, enlarged image of boxed area (*left*). *C*, biochemical analysis of mitochondrial function in arsenic-exposed A_L cells. Lysates from cells treated with arsenic (1 $\mu\text{g}/\text{mL}$) for 60 d were tested for COX and citrate synthase function by measuring the quantity of cytochrome *c* (nmol) oxidized per minute per mg protein and oxaloacetate (nmol) transformed per minute per mg protein. *Columns*, average from duplicate determinations from at least five clones; *bars*, SE. **, $P < 0.005$, Student's *t* test. Rates of oxygen consumption for intact A_L cells treated with arsenic (1 $\mu\text{g}/\text{mL}$) for 60 d and $\rho 0$ A_L cells with depleted mtDNA were determined using an oxygen electrode unit. *Columns*, average of duplicate determinations from two or three clones; *bars*, SE. Treatment of A_L cells with sodium arsenite decreases COX function and oxygen consumption but increases citrate synthase function.

Figure 4. mtDNA is depleted after sodium arsenite treatment. *A*, ethidium bromide-stained gel showing ~16-kb PCR amplified products of mtDNA from arsenic-treated cells and controls. Each lane represents long-extension PCR using as a template DNA extracted from independent cultures of A_L cells (*lane 1*) and cells treated with 0 $\mu\text{g}/\text{mL}$ (*lanes 2 and 3*), 0.25 $\mu\text{g}/\text{mL}$ (*lanes 4 and 5*), 0.5 $\mu\text{g}/\text{mL}$ (*lanes 6 and 7*), and 1 $\mu\text{g}/\text{mL}$ (*lanes 8 and 9*) sodium arsenite for 16 d. *B*, mtDNA copy number was determined by comparing the ratio of mtDNA to nDNA amplified using real-time quantitative PCR on extracts from cells exposed to arsenite for 60 d as well as controls. Columns, averages of two experiments done on extracts from each of two independent cell cultures; bars, SD. *, $P < 0.05$; **, $P < 0.005$, Student's *t* test compared with untreated controls.



(Fig. 2A). In contrast, cultures exposed to 1 $\mu\text{g}/\text{mL}$ arsenic for 60 days had a distribution of mitochondria that varied considerably between cells and exhibited a dramatically elongated or filamentous morphology (Fig. 2C). This extended mitochondrial morphology was also evident in cells stained histochemically for COX after only 15 days of arsenic exposure (Fig. 3B, arrow). We quantified this change in morphology by capturing images of randomly chosen fields and scoring the numbers of cells displaying an elongated, filamentous mitochondrial structure. In untreated cultures, only 6% of cells (SD, 7%) displayed an elongated mitochondrial morphology (6 fields, 230 cells), whereas for arsenic-treated cells 66% of cells (SD, 29%; $P < 0.01$, Student's *t* test) had this morphology (10 fields, 263 cells).

Arsenic treatment has been shown to degrade the microtubule aster (27, 28), and mitochondrial transport uses microtubules as "rails" and the associated microtubule motor proteins for motility, at least in mammalian cells (29, 30). It was possible that the degradation of the microtubule cytoskeleton would also alter mitochondrial phenotype within cell. However, we were unable to identify any gross phenotypic changes in the microtubule cytoskeleton in chronically treated cells (Fig. 2B and D).

Having identified a change in mitochondrial phenotype, we examined the effect of arsenic on mitochondrial metabolic activity. COX is a 13-subunit enzyme located in the inner mitochondrial membrane (29). Also known as complex IV in the respiratory chain, COX activity is routinely used as a measure of mitochondrial metabolic function. Interestingly, histochemical analysis of cells treated with arsenic for 15 days revealed a reduction in COX staining

compared with control cells (Fig. 3A and B), indicating that mitochondrial respiration was reduced after arsenic treatment. To quantify the histochemical data, we analyzed the absorbance of at least 23 randomly chosen cells from images of treated and untreated samples. After subtracting the background, the average absorbance (\pm SD) of images of untreated cells was 1.9 (\pm 0.2) times greater than for treated cells, indicating that untreated cells stained more heavily for COX, suggesting greater activity.

We next assayed biochemically COX activity on lysates from clonal isolates of arsenic-treated and untreated A_L cells. Significantly, COX activity was reduced by almost 45% after sodium arsenite treatment for 60 days (Fig. 3C). This confirmed our histochemical data and indicated that exposure to the metalloid reduced mitochondrial respiratory function. To further confirm that arsenite treatment compromised mitochondrial function, we assayed oxygen consumption in both control and arsenite-treated (1 $\mu\text{g}/\text{mL}$ for 60 days) A_L cells. Compared with nontreated controls, there was a 36% decrease in oxygen consumption among arsenite-treated A_L cells (Fig. 3C). As expected, $\rho 0$ A_L cells with depleted mtDNA had extremely low rates of oxygen consumption, 12 times less than wild-type A_L cells.

COX is the final enzyme in the respiratory chain and is composed of both nuclear and mitochondrial-encoded proteins. Thus, we compared the activity of citrate synthase, a wholly nuclear encoded mitochondrial matrix enzyme that is a measure of mitochondrial mass (31), with COX activity in the same lysates. Unexpectedly, there was a reciprocal increase in citrate synthase activity in response to arsenic treatment (Fig. 3C).

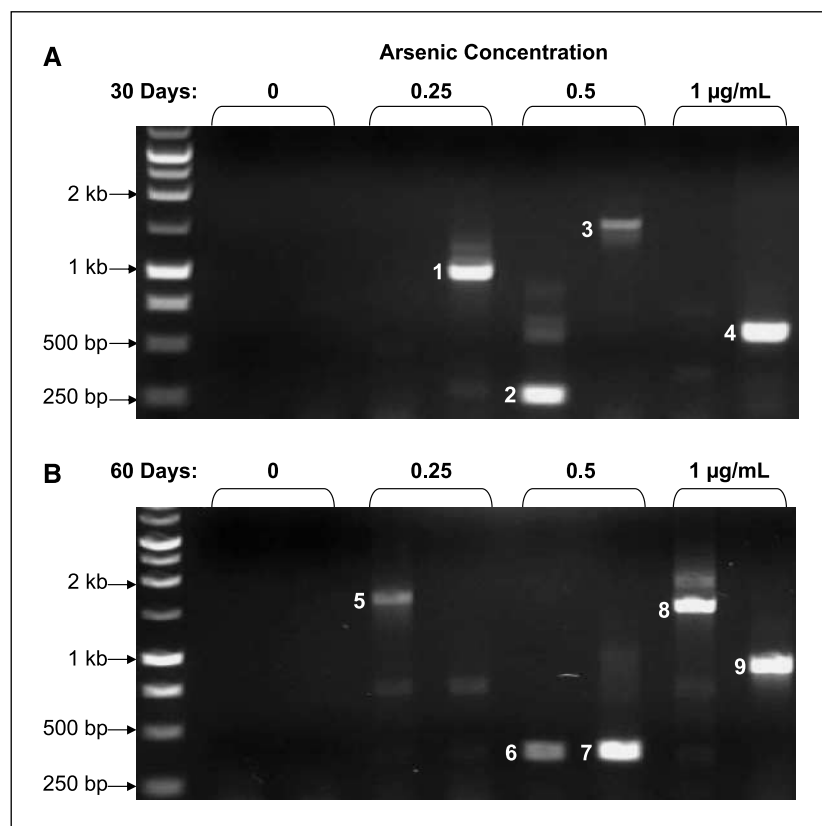


Figure 5. Large heteroplasmic deletions occur in mtDNA after arsenic treatment. *A* and *B*, 0.9% agarose gel of PCR products from second round of amplification of a nested PCR using DNA from A_L cells treated with arsenic for 30 d (*A*) and 60 d (*B*) at the indicated doses as a template for the first round of PCR. Duplicate cultures were screened for each treatment condition. The first round of nested PCR was done with primers 6123 sense + 14617 antisense (see Materials and Methods) using DNA isolated from cultures as a template. No products were visible (data not shown). The second round of PCR was done with primers 6716 sense + 14154 antisense and 1 μ L of first reaction used as a template. Nucleotide position of deletions in numbered bands are given in Table 1.

mtDNA alterations. COX is a complex with 3 of its 13 subunits encoded by mtDNA (32). It was possible that the decrease in COX activity after arsenic treatment resulted from mtDNA damage. There are at least two ways in which mtDNA could be altered after arsenic treatment: by depleting the copy number or by deleting sections of the genome. In an initial screen to identify mtDNA deletions, we used long-extension PCR to amplify almost the entire 16,284-bp A_L cell mitochondrial genome. However, fragments shorter than wild-type mtDNA (less than \sim 16 kb) were not detected (Fig. 4A), indicating that any deletions were likely to be heteroplasmic, affecting only a small fraction of the mtDNA copies present in the cell and, therefore, not detectable.

Surprisingly, even after shorter treatment time (15 days), there was a substantial decrease in ethidium bromide staining of the long-extension mtDNA PCR product in A_L cells treated with 1 μ g/mL arsenic compared with untreated samples or cells treated with lower doses (Fig. 4A, lanes 8 and 9), despite using equivalent quantities of template DNA. This suggested that mtDNA copy number may be reduced. To confirm this result, we did real-time quantitative PCR. Segments from both mtDNA and nDNA were amplified, and the relative mtDNA to nDNA ratio was assessed in arsenic-treated cells compared with untreated controls. The two fragments amplified were from the hamster *12S* rRNA gene, a highly conserved region of the mitochondrial genome (24), and a segment of the nuclear-encoded *18S* rRNA gene (23). Interestingly, after 60 days of arsenic treatment, mtDNA copy number was reduced to <65% of untreated levels. This effect was dose dependent and was observed in cells exposed to arsenic concentration of 0.5 μ g/mL. mtDNA copy number was also reduced in cells treated with arsenic at 0.25 μ g/mL, although the effect at this dose was not statistically significant (Fig. 4B).

Having confirmed changes in mtDNA after arsenic exposure, we used a more sensitive method to detect rare heteroplasmic mtDNA deletions. In humans, a PCR-based technique had been developed to detect heteroplasmic deletions that exploited the physical characteristics of a circular mtDNA molecule containing a large deleted fragment (26). Primer annealing sites in the wild-type mitochondrial genome that were thousands of base pairs apart would be substantially closer together after deletion of the intervening sequence and re-circularization of the genome. Using short extension times (30 s), it has been shown that the sequences flanking the deleted fragment would be selectively amplified even when present as a fraction of the total mtDNA copy number.

In humans, the vast majority of mtDNA deletions that have been identified thus far occur between tandem repeats, including the "common" deletion (33).⁴ In addition, 85% of the deletions flanked by direct repeats observed in humans are contained completely within the major arc (the larger, \sim 11,000 bp, of the two sequences between O_H and O_L in the circular mitochondrial genome; ref. 33). In hamster mtDNA, there are a large number of repeats in the major arc of 11 bp or longer (Supplementary Table S1). Using a pair of nested primer sets, the PCR procedure for detecting the "common" deletion in humans was adapted to hamster mtDNA in an attempt to identify large deletions.

Duplicate cultures were exposed to 0.25, 0.5, and 1 μ g/mL arsenic for 30 days and analyzed for deletions using two different

⁴ MITOMAP. A Human Mitochondrial Genome Database (<http://www.mitomap.org>), 2006.

sets of nested primers. Surprisingly, after arsenic exposure large heteroplasmic deletions were detected by PCR amplification of fragments in A_L cell mtDNA that were not found in untreated cells (Fig. 5A). These results were further confirmed by sequencing the PCR products (Table 1). Deletions were observed even after short (24 h) treatment times with relatively low concentrations (0.25 $\mu\text{g}/\text{mL}$) of arsenic (Table 1). Unexpectedly, when we repeatedly assayed a single DNA sample extracted from an exposed culture, we identified many different deletion products (Table 1), indicating that multiple, possibly single copy, deletions were induced by arsenic treatment. Consistent with this finding, the DNA from the same continuously cultured cells when analyzed

after 60 days of arsenic exposure displayed deletions that were not detected after 30 days of treatment (Fig. 5B). Deletions were also not detected in arsenic-treated $\rho 0 A_L$ cells, indicating that they were not due to pseudogenes present in nDNA (data not shown).

Discussion

In this study, we observed a reduction in mtDNA copy number, an increased incidence of large heteroplasmic deletions, a reduction of COX activity, and an increase in citrate synthase activity, indications that mitochondrial replication and function were abnormal after arsenic treatment. This suggests that exposed

Table 1. Deletions detected in arsenic treated A_L cells by nested PCR

Arsenic exposure		Primers*	Deletion [†]	Tandem repeat [‡]
Time (d)	Dose ($\mu\text{g}/\text{mL}$)			
1	0.25	α	5805-10964	CAATCA
1	0.25	α	5936-10617	ATTACTA
1	0.5	α	5704-11207	—
1	0.5	α	5241-11291	—
1	0.5	β	6915-13779	—
1	1.0	α	5977-11206	—
1	1.0	α	5671-10689	—
1	1.0	β	7706-13479	TTTA
1	1.0	β	6989-13645	—
15	2.0	α	6095-11253	—
15	2.0	β	7147-13600	—
15	2.0	α	5765-11006 ^x	CACTTA
15	2.0	α	5635-10876 ^x	—
15	2.0	α	5794-11007 ^x	TATT
15	2.0	α	5700-11329 ^x	ATTAG
15	2.0	α	5863-11313 ^x	TGATC
15	2.0	α	5623-11077 ^x	—
15	2.0	α	6085-11086 ^x	—
15	2.0	α	5895-11284 ^x	ATTACT
15	2.0	α	5643-11218 ^x	—
15	2.0	α	5636-10837 ^x	—
15	2.0	α	5862-11368 ^x	—
30	0.25	β	6880-13286 ¹	—
30	0.25	α	5781-11180	—
30	0.5	α	5823-10600	—
30	0.5	β	6909-14073 ²	CTATG
30	0.5	β	8004-13836 ³	TGACAT
30	1.0	α	5879-11208	—
30	1.0	α	6217-11386 ^y	—
30	1.0	α	7100-10918 ^y	—
30	1.0	α	6675-10719 ^y	—
30	1.0	β	7035-13909 ⁴	CACC
60	0.25	β	6756-12515 ⁵	—
60	0.5	β	7027-14097 ⁷	—
60	0.5	β	6981-14030 ⁶	—
60	1.0	β	7393-13789	—
60	1.0	β	6933-12832 ⁸	—
60	1.0	β	7128-13644 ⁹	—

* Primer sets: α , 5070S + 11775AS and 5700S + 11387AS; β , 6123 + 14617 and 6716 + 14154.

[†] Nucleotide numbering from Partridge et al. (24). Superscripted numbers correspond to bands in Fig. 5. Superscripted letters indicate different deletions identified from the same sample.

[‡] Repeats greater than 3 bp either overlapping or adjacent.

cells have moved from an oxidative toward a glycolytic metabolic state. Interestingly, the Warburg theory, advanced many decades ago (6), implies that cancer cells also have impaired mitochondrial function and increased glycolysis. In addition, the “mitochondrial dysfunction hypothesis” contends that the three deleterious features (increased oxidative stress, energy deprivation, and mtDNA damage) contribute to a degenerative cycle and thus compound the effect of each of the other factors individually (18). At least two of these factors, increased ROS and mtDNA depletion, have been previously implicated in DNA damage and genotoxicity after arsenic exposure (4, 17). In addition to our previous work, we have now shown here that all three factors (including mitochondrial dysfunction, mtDNA depletion, and induction of mtDNA deletions) are observed after arsenic treatment of cells, and it is possible that a related degenerative cycle of mitochondrial dysfunction may contribute to the carcinogenicity of arsenic in humans. These data support the theory that the mitochondria, and particularly mtDNA, are important mediators of the mutagenic effects of arsenic in mammalian cells.

It should be noted that although the concentrations of arsenic in this study are high compared with average exposure levels observed in affected communities, in Bangladesh and parts of West Bengal, India, >30% of drinking wells have arsenic levels greater than 100 µg/L, and 5% to 10% of wells have levels between 200 and 1,000 µg/L (2, 34). These concentrations are well within the dosage range used in the experiments reported here. In addition, the experiments in this study were conducted for at most 60 days, a dramatically shorter period than the chronic exposure experienced in affected communities. Consequently, we believe that the arsenic levels used here effectively simulate conditions that are environmentally relevant.

Our initial experiments confirmed that arsenic was a genotoxic mutagen and also induced genomic instability, measured by an increase in micronuclei (5). The induction of micronuclei had been previously observed in free radical-sensitive cells exposed to very high arsenic concentrations (35). Our analysis revealed an increase in micronuclei in normal cells after arsenic treatment at much lower doses, reinforcing the concept that arsenic is a potent chromosomal mutagen. In comparison with our previous studies of arsenic-treated A_L cells, there was a modest increase in survival fraction and a reduction in mutation yield (4). It is possible that the serial passaging required to continuously treat cells for more than 1 week may have affected these results, as could variability in complement used in the mutation assay.

In addition to examining nuclear genotoxicity, we wanted to understand the effects of arsenic on mitochondrial respiratory chain function and, in particular, whether arsenic induced damage in mtDNA. Histochemical analysis of COX activity revealed a decrease in staining of arsenic-treated cells, suggesting a reduced respiratory chain function. This was confirmed by biochemical analysis that showed that COX activity was decreased by nearly 45% after arsenic treatment. This was consistent with our previous observation that arsenic induced the formation of peroxynitrites (5), as these molecules inhibit COX (complex IV), as well as complexes I, II, and V (36). Arsenic treatment also reduced oxygen consumption in chronically exposed A_L cells, supporting the evidence of reduced COX activity. A reduced rate of oxygen consumption has previously been reported in cells treated acutely with arsenic as well as in chronically exposed animals (37, 38).

We also examined citrate synthase activity, an enzyme that is encoded by nuclear genes and found that the effect of arsenic on the

enzyme was the reciprocal of the effect on COX. Citrate synthase activity is inhibited by ATP, thus providing an important regulatory mechanism to control the citric acid cycle (39). In arsenic-treated cells that had decreased COX activity, ATP production (the end product of the electron transport chain) was likely to be reduced. Consequently, the relative reduction in ATP concentration in these cells may have resulted in a compensatory increase in citrate synthase activity compared with controls.

We and others have shown that direct mutations to specific nuclear genes (*CD59*), as well as genomic instability (micronucleus formation), was clearly induced by arsenic exposure, and these effects could be ameliorated by reducing the levels of ROS in the cell (4, 35). These findings, combined with the decrease in COX activity in arsenic-treated cells, prompted us to examine the integrity of the mitochondrial genome.

There were a number of ways in which mtDNA could be altered, one of which was a reduction in the copy number. There are many hundreds of copies of the mitochondrial genome in any given cell, and a reduction in copy number may affect the expression level of the three COX subunits encoded by mtDNA. This, in turn, could alter the activity of complex IV as a whole, which may increase the level of ROS. Significantly, there was evidence that cancer cells (HeLa) with depleted mtDNA have impaired DNA repair capacity and increased oxidative damage to the nuclear genome (17). These results were reinforced by our previous findings of increased background *CD59* mutation levels in ρ0 A_L cells, a CHO-derived, non-tumor cell line (5).

In our experiments, we observed a clear decrease in the ratio of mtDNA to nDNA when cells were treated with 1 µg/mL arsenic. After longer-term exposures (up to 60 days), cells displayed a dose-dependent reduction of mtDNA copy number, indicating that lower concentrations of arsenic, more similar to the average environmental exposure levels experienced in drinking water, also caused a reduction in copy number. It has been reported that mRNA expression of DNA polymerase-γ, the polymerase responsible for the replication and repair of mtDNA, is substantially reduced in arsenic-treated cultures, and this could account for the reduction in mtDNA (40). Alternatively, the reduction of mtDNA copy number may be a consequence of the increase in free radicals in exposed cultures. ROS-induced damage to DNA polymerase-γ, in addition to a decrease in mRNA expression, could have further impaired replication of the mitochondrial genome, thus reducing the copy number. In support of this concept, it has been established that DNA polymerase-γ is susceptible to oxidative damage *in vitro* (41).

Perhaps the most interesting finding of this work was the evidence that large heteroplasmic deletions in the mitochondrial genome were induced by arsenic exposure. The genome was apparently subjected to repeated damage, as a number of unique deletions were detected in mtDNA from each sample, as well as mtDNA extracted at different times from the same continuously cultured cell line. Furthermore, the observation that mtDNA deletions were present after 24 h of exposure was consistent with our previous observations that arsenic-induced nuclear genotoxicity occurred within 24 h (4, 5).

Of the deletions identified, less than one third (11 of 38) were located adjacent to tandem repeats. However, in humans, the vast majority of identified deletions are flanked by tandem repeats.⁴ This discrepancy may be accounted for by the fact that deletions flanked by tandem repeats are more likely to be propagated to higher percentage levels in an individual cell and hence become

fixed, and therefore more readily detectable in humans, whereas other deletions are repaired/degraded or not amplified. The detection of deletions in arsenic-treated cells likely reveals an increase in the incidence of these mutations after exposure, not their complete absence in unexposed cells. The ability to detect deletions in treated cells may be explained by a number of factors: increased ROS resulting in more double-strand breaks, decreased DNA repair capacity or a lower mitotic index, as human tissues with a low mitotic index have an increased incidence of the common deletion (42, 43). Regardless of the mechanism by which deletions were induced, our data indicate that the mitochondrial genome was subjected to repeated and continuous damage when exposed to arsenic.

Arsenic is an important environmental contaminant that affects millions of people worldwide. Our present findings illustrate that mitochondria are a primary target in arsenic toxicity and provide a basis for better interventional approach in both treatment and prevention of arsenic-induced human diseases.

Acknowledgments

Received 1/5/2007; revised 3/2/2007; accepted 4/4/2007.

Grant support: NIH grants ES 05786 and ES 12888, Superfund grant P42 ES 10349, and Environmental Center grant ES 09089.

The costs of publication of this article were defrayed in part by the payment of page charges. This article must therefore be hereby marked *advertisement* in accordance with 18 U.S.C. Section 1734 solely to indicate this fact.

We thank Winsome Walker and Sindu Krishna for expert technical assistance.

References

- Parvez F, Chen Y, Argos M, et al. Prevalence of arsenic exposure from drinking water and awareness of its health risks in a Bangladeshi population: results from a large population-based study. *Environ Health Perspect* 2006;114:355–9.
- Smith AH, Lingas EO, Rahman M. Contamination of drinking-water by arsenic in Bangladesh: a public health emergency. *Bull World Health Organ* 2000;78:1093–103.
- Ahsan H, Chen Y, Parvez F, et al. Health Effects of Arsenic Longitudinal Study (HEALS): description of a multidisciplinary epidemiologic investigation. *J Expo Sci Environ Epidemiol* 2006;16:191–205.
- Hei TK, Liu SX, Waldren C. Mutagenicity of arsenic in mammalian cells: role of reactive oxygen species. *Proc Natl Acad Sci U S A* 1998;95:8103–7.
- Liu SX, Davidson MM, Tang X, et al. Mitochondrial damage mediates genotoxicity of arsenic in mammalian cells. *Cancer Res* 2005;65:3236–42.
- Warburg O. On respiratory impairment in cancer cells. *Science* 1956;124:269–70.
- Liu SX, Athar M, Lippai I, Waldren C, Hei TK. Induction of oxyradicals by arsenic: implication for mechanism of genotoxicity. *Proc Natl Acad Sci U S A* 2001;98:1643–8.
- Wei YH. Oxidative stress and mitochondrial DNA mutations in human aging. *Proc Soc Exp Biol Med* 1998;217:53–63.
- Croteau DL, Stierum RH, Bohr VA. Mitochondrial DNA repair pathways. *Mutat Res* 1999;434:137–48.
- von Wurmb-Schwark N, Higuchi R, Fenech AP, et al. Quantification of human mitochondrial DNA in a real time PCR. *Forensic Sci Int* 2002;126:34–9.
- Cortopassi GA, Arnheim N. Detection of a specific mitochondrial DNA deletion in tissues of older humans. *Nucleic Acids Res* 1990;18:6927–33.
- von Wurmb-Schwark N, Cavelier L, Cortopassi GA. A low dose of ethidium bromide leads to an increase of total mitochondrial DNA while higher concentrations induce the mtDNA 4997 deletion in a human neuronal cell line. *Mutat Res* 2006;596:57–63.
- Lee HC, Yin PH, Yu TN, et al. Accumulation of mitochondrial DNA deletions in human oral tissues: effects of betel quid chewing and oral cancer. *Mutat Res* 2001;493:67–74.
- Jessie BC, Sun CQ, Irons HR, Marshall FF, Wallace DC, Petros JA. Accumulation of mitochondrial DNA deletions in the malignant prostate of patients of different ages. *Exp Gerontol* 2001;37:169–74.
- Chatterjee A, Mambo E, Sidransky D. Mitochondrial DNA mutations in human cancer. *Oncogene* 2006;25:4663–74.
- Bianchi MS, Bianchi NO, Bailliet G. Mitochondrial DNA mutations in normal and tumor tissues from breast cancer patients. *Cytogenet Cell Genet* 1995;71:99–103.
- Delsite RL, Rasmussen LJ, Rasmussen AK, Kalen A, Goswami PC, Singh KK. Mitochondrial impairment is accompanied by impaired oxidative DNA repair in the nucleus. *Mutagenesis* 2003;18:497–503.
- Lewis W, Copeland WC, Day BJ. Mitochondrial DNA depletion, oxidative stress, and mutation: mechanisms of dysfunction from nucleoside reverse transcriptase inhibitors. *Lab Invest* 2001;81:777–90.
- Alirol E, Martinou JC. Mitochondria and cancer: is there a morphological connection? *Oncogene* 2006;25:4706–16.
- Salviati L, Hernandez-Rosa E, Walker WF, et al. Copper supplementation restores cytochrome *c* oxidase activity in cultured cells from patients with SCO2 mutations. *Biochem J* 2002;363:321–7.
- Partridge MA, David FS, Marcantonio EE. Displacement of the β -cytoplasmic domain recovers focal adhesion formation, cytoskeletal organization and motility in swapped integrin chimeras. *J Cell Sci* 2006;119:1175–83.
- King MP, Koga Y, Davidson M, Schon EA. Defects in mitochondrial protein synthesis and respiratory chain activity segregate with the tRNA(Leu)(UUR) mutation associated with mitochondrial myopathy, encephalopathy, lactic acidosis, and stroke-like episodes. *Mol Cell Biol* 1992;12:480–90.
- Wejksnora PJ, Dumenco VM, Bacsí SG. Fragments of rDNA within the Chinese hamster genome. *Biochem Genet* 1988;26:19–35.
- Partridge MA, Davidson MM, Hei TK. The complete nucleotide sequence of Chinese hamster (*Cricetulus griseus*) mitochondrial DNA. *DNA Seq*. In press 2007.
- Shao G, Berenguer J, Borczuk AC, Powell CA, Hei TK, Zhao Y. Epigenetic inactivation of Betaig-h3 gene in human cancer cells. *Cancer Res* 2006;66:4566–73.
- Soong NW, Arnheim N. Detection and quantification of mitochondrial DNA deletions. *Methods Enzymol* 1996;264:421–31.
- Wang YC, Chung RH, Tung LC. Comparison of the cytotoxicity induced by different exposure to sodium arsenite in two fish cell lines. *Aquat Toxicol* 2004;69:67–79.
- Ramirez T, Garcia-Montalvo V, Wise C, Cea-Olivares R, Poirier LA, Herrera LA. *S*-adenosyl-L-methionine is able to reverse micronucleus formation induced by sodium arsenite and other cytoskeleton disrupting agents in cultured human cells. *Mutat Res* 2003;528:61–74.
- DiMauro S, Schon EA. Mitochondrial respiratory-chain diseases. *N Engl J Med* 2003;348:2656–68.
- Fuchs F, Prokisch H, Neupert W, Westermann B. Interaction of mitochondria with microtubules in the filamentous fungus *Neurospora crassa*. *J Cell Sci* 2002;115:1931–7.
- Nishigaki Y, Marti R, Copeland WC, Hirano M. Site-specific somatic mitochondrial DNA point mutations in patients with thymidine phosphorylase deficiency. *J Clin Invest* 2003;111:1913–21.
- Dimauro S, Davidzon G. Mitochondrial DNA and disease. *Ann Med* 2005;37:222–32.
- Samuels DC, Schon EA, Chinnery PF. Two direct repeats cause most human mtDNA deletions. *Trends Genet* 2004;20:393–8.
- Rahman MM, Sengupta MK, Ahamed S, et al. Arsenic contamination of groundwater and its health impact on residents in a village in West Bengal, India. *Bull World Health Organ* 2005;83:49–57.
- Wang TS, Huang H. Active oxygen species are involved in the induction of micronuclei by arsenite in XRS-5 cells. *Mutagenesis* 1994;9:253–7.
- Brown GC. Nitric oxide as a competitive inhibitor of oxygen consumption in the mitochondrial respiratory chain. *Acta Physiol Scand* 2000;168:667–74.
- Bencko V, Nemeckova H. Oxygen consumption by mouse liver homogenate during drinking water arsenic exposure. *I J Hyg Epidemiol Microbiol Immunol* 1971;15:104–10.
- Pellicano H, Feng L, Zhou Y, et al. Inhibition of mitochondrial respiration: a novel strategy to enhance drug-induced apoptosis in human leukemia cells by a reactive oxygen species-mediated mechanism. *J Biol Chem* 2003;278:37832–9.
- Harford S, Weitzman PD. Evidence of isosteric and allosteric nucleotide inhibition of citrate synthase from multiple-inhibition studies. *Biochem J* 1975;151:455–8.
- Andrew AS, Warren AJ, Barchowsky A, et al. Genomic and proteomic profiling of responses to toxic metals in human lung cells. *Environ Health Perspect* 2003;111:825–35.
- Graziewicz MA, Day BJ, Copeland WC. The mitochondrial DNA polymerase as a target of oxidative damage. *Nucleic Acids Res* 2002;30:2817–24.
- Lee HC, Pang CY, Hsu HS, Wei YH. Differential accumulations of 4,977 bp deletion in mitochondrial DNA of various tissues in human ageing. *Biochim Biophys Acta* 1994;1226:37–43.
- Cortopassi GA, Shibata D, Soong NW, Arnheim N. A pattern of accumulation of a somatic deletion of mitochondrial DNA in aging human tissues. *Proc Natl Acad Sci U S A* 1992;89:7370–4.

Cancer Research

The Journal of Cancer Research (1916–1930) | The American Journal of Cancer (1931–1940)

Arsenic Induced Mitochondrial DNA Damage and Altered Mitochondrial Oxidative Function: Implications for Genotoxic Mechanisms in Mammalian Cells

Michael A. Partridge, Sarah X.L. Huang, Evelyn Hernandez-Rosa, et al.

Cancer Res 2007;67:5239-5247.

Updated version	Access the most recent version of this article at: http://cancerres.aacrjournals.org/content/67/11/5239
Supplementary Material	Access the most recent supplemental material at: http://cancerres.aacrjournals.org/content/suppl/2007/06/01/67.11.5239.DC1

Cited articles	This article cites 42 articles, 14 of which you can access for free at: http://cancerres.aacrjournals.org/content/67/11/5239.full.html#ref-list-1
Citing articles	This article has been cited by 6 HighWire-hosted articles. Access the articles at: /content/67/11/5239.full.html#related-urls

E-mail alerts	Sign up to receive free email-alerts related to this article or journal.
Reprints and Subscriptions	To order reprints of this article or to subscribe to the journal, contact the AACR Publications Department at pubs@aacr.org .
Permissions	To request permission to re-use all or part of this article, contact the AACR Publications Department at permissions@aacr.org .